This project is supported by the European Commission's FP7 Capacities Programme for the period April 2013 - March 2017 under the Grant Agreement number 312495.

www.solarnet-east.eu

DELIVERABLE D70.5

GREGOR Heat Rejecter Prototype and Test Report

WP70 Wavefront Control: Turbulence Characterization and Correction

1ST Reporting Period

November 2014

This project is supported by the European Commission's FP7 Capacities Programme for the period April 2013 - March 2017 under the Grant Agreement number 312495.

PROJECT GENERAL INFORMATION

Grant Agreement number: 312495

Project acronym: SOLARNET

Project title: High-Resolution Solar Physics Network

Funded under: FP7-INFRASTRUCTURES: INFRA-2012-1.1.26 - Research Infrastructures for High-Resolution Solar Physics

Funding scheme: Combination of Collaborative Project and Coordination and Support Action for Integrating Activities

From: 2013-04-01 to 2017-03-31

Date of latest version of Annex I against which the assessment will be made: **13/02/2013**

Periodic report: 1st **X** 2nd ☐ 3rd ☐ 4th ☐

Period covered: from **01/04/2013** to **30/09/2014**

Project's coordinator: Dr. Manuel Collados Vera, IAC.

Tel: (34) 922 60 52 00

Fax: (34) 922 60 52 10

E-mail: mcv@iac.es

Project website address: http://solarnet-east.eu/

S.R.S. Engineering Design S.r.l

SOLARNET
GREGOR Heat Rejecter Prototype Design Report

SRSED Code	Type	Release
317000_S1DV01_01	DV	1

Contract	Client	EU
	Reference	FP7, INFRA-2012-1.1.26, Grant No. 312495 (SOLARNET)
	WP	WP70.3.2/a
Object	**GREGOR Heat Rejecter Prototype Design Report**	
Other Information	This is the Deliverable D70.5 (GREGOR Heat Rejecter prototype and test report). At the beginning terms and results of Heat Rejecter Thermal and Hydraulic Design are presented. Then the corresponding Mechanical Detailed Design is shown. At last, the Interchangeable Field-Stop subsystem is described.	

Distribution list

1	21/09/2014	First Issue			
			A. Scotto	***F. Manni***	***L. Gramiccia***
Rev.	**Date**	**Object**	**Prepared**	**Verified**	**Approved**

Record of Revisions

Rev.	date	description	Notes
1	21/09/2014	First issue	

Index

List of Figures

List of Tables

1 REFERENCE DOCUMENTS

2 ACRONYMS

acronym	description
ASAP	As Soon As Possible
FS	Field-Stop (diaphragm)
FW	First Wall (HR reflecting surface, i.e. M1 side)
HR	Heat Rejecter
HTC	Heat Transfer Coefficient
JP	Jet Impingement
KIS	Kiepenheuer-Institut für Sonnenphysik
LOCA	Loss of Coolant Accident
LOFA	Loss of Flow Accident
q”	Surface Heat Flux (Heat Flow per unit area)
SRSED	S.R.S. Engineering Design s.r.l.
TBC	To Be Confirmed

Table 1 - Acronyms

3 REFERENCES

Ref. 1 – Manni (SRSED), Fischer (KIS) , ED317000_S1TN01_01.doc, Design Input Data
Ref. 2 – Viswanath Ravindranath, Sushil Sharma, Brian Rusthoven APS (Argonne National Laboratory, 9700 S. Cass Ave., Argonne, IL 60439, USA), Michael Gosz (Illinois Institute of Technology, 3300 S. Federal St., Chicago, IL 60616, USA), Lin Zhang, Jean-Claude Biasci (ESRF, BP-220, 6, rue Jules Horowitz, 38043 Grenoble Cedex 09, France), "Thermal Fatigue Life Prediction of Glidcop® Al-15"
Ref. 3 – John H. Lienhard, Joachim Hadeler, "High heat Flux Cooling by Liquid Jet-Array Modules", Chem. Eng. Technol. 22 (1999) 11
Ref. 4 – Joseph Milnes, "Computational Modelling of the HyperVapotron Cooling Technique for Nuclear Fusion", Department of Aerospace Sciences, Cranfield University, Cranfield, UK, 2010
Ref. 5 – C.T. Chang, G. Kojasoy, F. Landis (Department od Mechanical Engineering Univeristy of Wisconsin-Milwaukee, WI 53201, U.S.A.), S. Dowing (Sundstrand Corporation, 4747 Harrison Avenue, Rockford, IL 61125, U.S.A.), "Confined single- and multiple-jet impingement heat transfer – I. Turbulent submerged liquid jets", Int. J. Heat Mass Transfer. Vol. 38, No. 5, 1995
Ref. 6 – Chin-Yuan Li, Suresh, V. Garimella, "Prandtl-number effects and generalized correlations for confined and submerged jet impingement", School of Mechanical Engineering, Purdue University, West Lafayette, IN 47907-1288, U.S.A., November 2000
Ref. 7 – S.V.J. Narumanchi, V. Hassani, and D. Bharathan, "Modeling Single-Phase and Boiling Liquid Jet Impingement Cooling in Power Electronics", National Renewable Energy Laboratory, Battelle, U.S.A., NREL/TP-540-38787, December 2005
Ref. 8 – "Flow of Fluids through Valves Fittings, and Pipe", CRANE CO., 1999

4 SUMMARY

This is the Deliverable D70.5 (GREGOR Heat Rejecter prototype and test report). At the beginning terms and results of Heat Rejecter Thermal and Hydraulic Design are presented. Then the corresponding Mechanical Detailed Design is shown. At last, the Interchangeable Field-Stop subsystem is described.

5 INPUT DATA

Starting from the content of the input data reference document (**Ref. 1**), optical, geometric, thermal-hydraulic, and safety designed constraints have been analyzed and detailed in the following sections.

5.1 Optical design

For the purposes of the activity a few information, limited to M1, M2, F1, F2 is required, which is summarized in Table 2.

M1	Primary mirror	shape	Parabolic
		Outer diameter	1.560 [m]
		Inner Diameter	0.380 [m]
		focus	2.5075 [m]
M2	Secondary mirror	shape	Elliptical
		Outer diameter	0.430 [m]
		1st focus (distance M2-F1)	0.668 [m]
		2nd focus (distance M2-F2)	2.314 [m]

Table 2 – GREGOR Optical design data

The corresponding optical scheme and the HR position is reported in Figure 1.

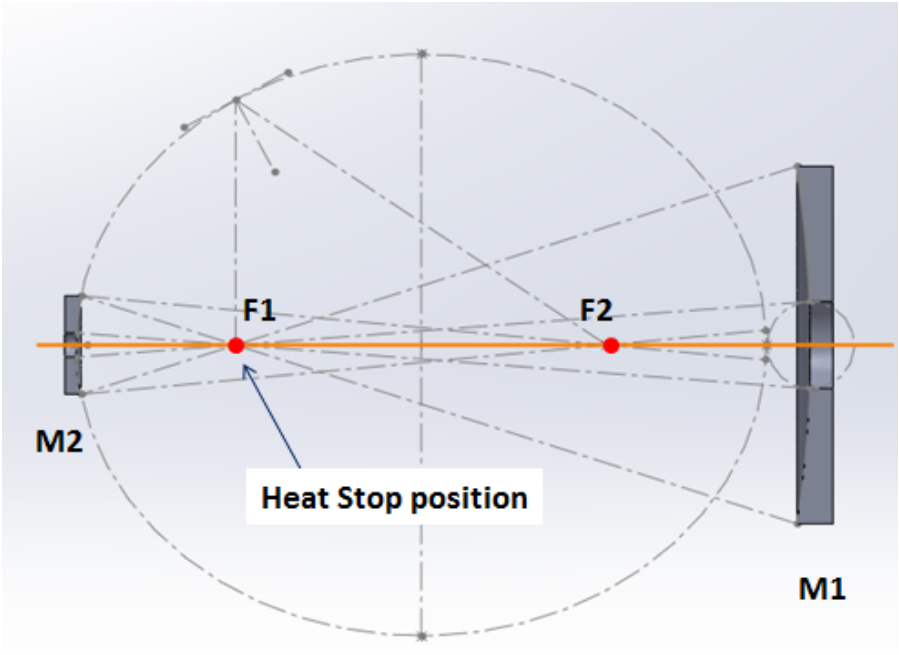

Figure 1 – GREGOR Optical Scheme

The optical scheme determines the zone which can host the HR without interfering with light reflected by M2 towards F2 (see next section).

5.2 HR bounding box

The space which is available for hosting the HR is a solid of revolution obtained by rotating the yellow triangle, shown in Figure 2-a, around the telescope axis. It features a slightly conical outer shape (exaggerated in Figure 2-b) with a minimum diameter of 72 [mm], but for safety reasons a cylindrical shape with a diameter of 65 [mm] has been chosen, equal to the outer diameter of the HR currently installed.

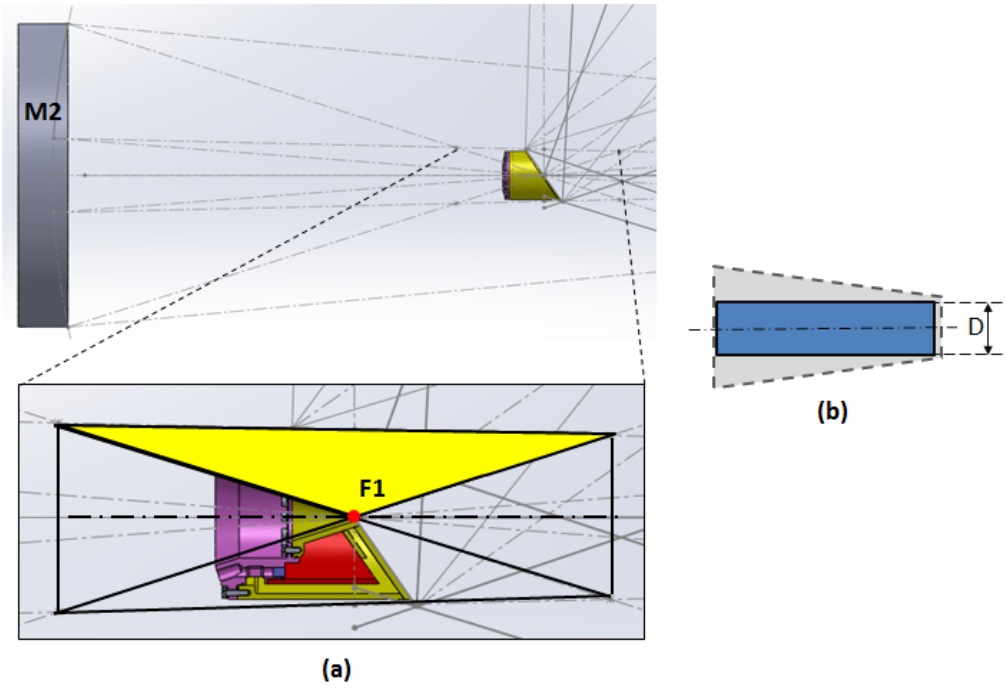

Figure 2 – HR bounding box

The theoretical inner cone angle is slightly greater than 35° (35.36°), but, again, for safety reasons, a value of 35° has been assumed. Regarding reflecting surface, an attempt was made to preserve the initial value of 37.5°, but, due to strong asymmetry, the internal part arrangement resulted to be quite critical, and a compromise value of 35° was chosen. The basic geometry (the "bounding box") to be used for the HR design is shown in Figure 3.

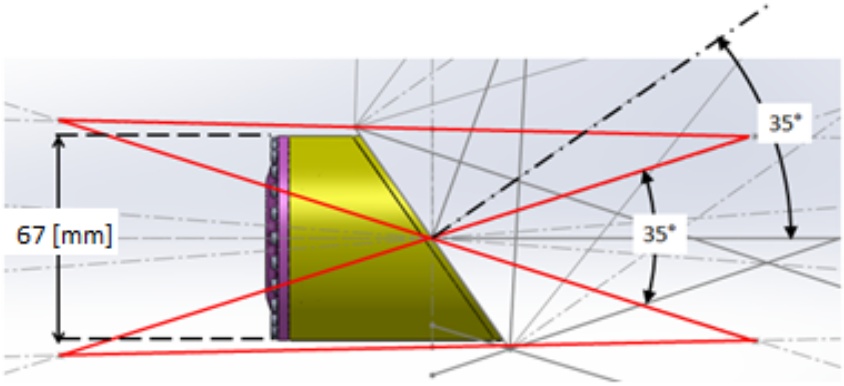

Figure 3 – HR basic geometry

5.3 Cooling System

The actual HR features a double coolant circuit shown in Figure 4.

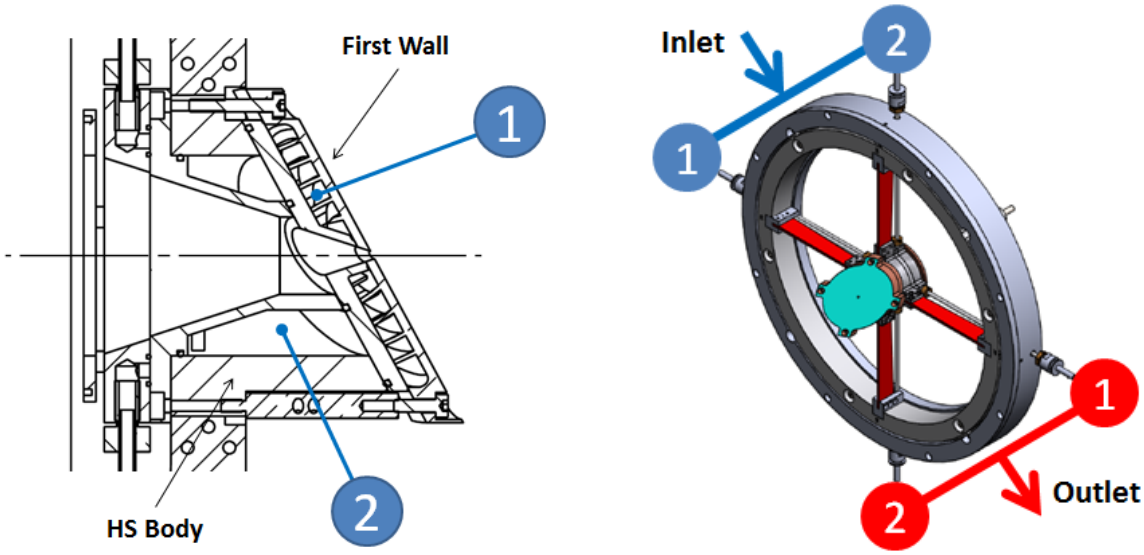

Figure 4 – Actual HR Cooling System

The most important and critical one serves the First Wall (the face illuminated by the sun light) which is cooled by the double-helical flow (from the border to the diaphragm hole, then back to the border) shown in Figure 5.

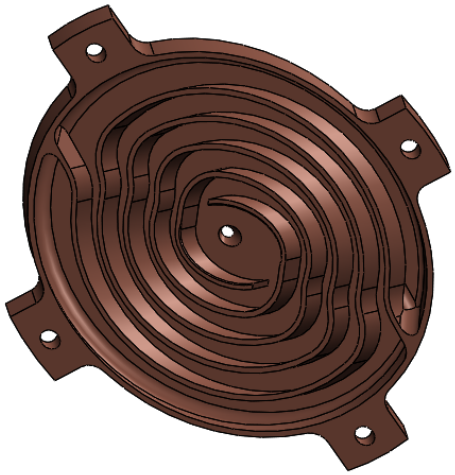

Figure 5 – Actual HR – FW Double-Helical flow duct

Another important aspect is the presence of the four Feeders ("Feeder Cross"), that is the pipes which feed/drain the water to/from the HR. Those Feeders have a fixed outer diameter (4 [mm]) which cannot be increased (they stay in the path of the reflected light from M2 to F2). If an increase of the Coolant Flow Rate were necessary (*as it will be*), in order to limit the coolant velocity inside the Feeders, only their number will be increased (doubled) by overlapping a second "Feeder Cross" in the shadow of the first one. Since the cooling concept adopted in the new HR is different from the actual one, substantial changes have been introduced (discussed later on).

5.4 Safety System

The purpose of the Safety System is to preserve di HR structure from the high temperatures which may be reached due to:

- Bad telescope pointing
- Cooling System Failure (LOCA: Loss of Coolant Accident, LOFA: Loss of Flow Accident)

In both cases the telescope cover must be closed ASAP (Shutdown). The closure is commanded by the following signals:

- T1 – (2, TBC) Temperature Sensors located inside the HR
- T3 – Temperature Sensor located on the HR Support Structure (the Ring)
- F1 – Flow meter at the HR outlet

Sensors monitored via Software (control program) and Hardware (Temperature and Flow Rate switch). The basic control logic is summarized in Table 3.

Sensor	Shutdown (Cover is closed and locked)	Cover unlocked	Notes
T1	T > 38°C (software) T > 40°C (hardware)	T < 35°C	
T3	$T > T_{amb}+10°C$	$T < T_{amb}+5°C$	The Ring is thermally insulated and, in normal condition, its temperature should be close to the ambient temperature (T_{amb})
F1	FR < 1.7 [l | m]	(TBC)	

Table 3 – Safety Control Logic

The same Safety Control logic will be maintained in the new HR, but it is possible that new set-points must be adopted for T1 due to the different design and then to the different thermal field. The actual arrangement for T1 sensors in shown in Figure 6.

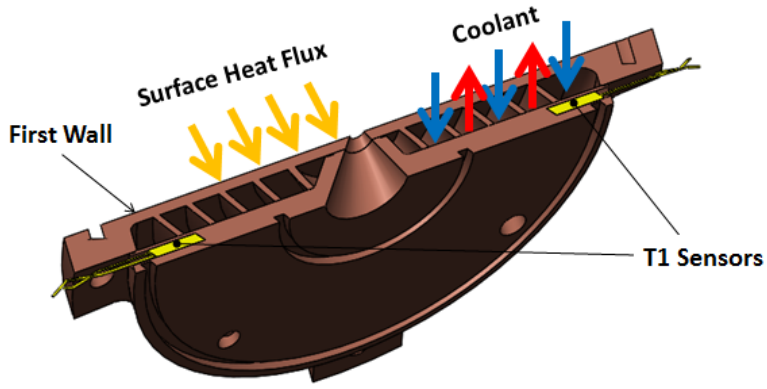

Figure 6 – Actual HR – T1 Temperature Sensor positions

6 HR THERMAL-HYDRAULIC DESIGN

The First Wall (FW) is the key part of the entire HR Thermal and Hydraulic Design. It is heavily irradiated by the Sun light concentrated by M1. The whole design process is aimed at keeping the FW temperature at reasonable low value. This implies reaching a very high Heat Transfer Coefficient (HTC) which can be attained by the adoption of the Jet Impingement technique.

6.1 Design Thermal Load

We will define the Thermal Load as the heat flux (heat flow per unit area) which must be sustained by the FW for an indefinite amount of time. For its own nature, no more than the defined thermal load will affect the component (i.e. it's the maximum conceivable). The value of the Design Thermal Load comes from the following assumptions:

- In terms of irradiance, it has been conservatively assumed that 900 [W|m^2] (out of the 1340 which would be seen without the atmosphere), impinge on M1, which correspond to a Heat Flow of about 1625 [W].
- Assuming a M1 reflectivity of 95% (good for M1, but bad for the HR), some 1543 [W] are reflected onto the HR. Assuming that a HR FW reflectivity of 85% (degraded coating), a resulting heat flow of some 232 [W] is absorbed by the HR and must be removed.
- Assuming that a radius of the solar image on the Focal Plane of 11.86 [mm], and applying a suitable correction due to the HR FW inclination (35°), a resulting Heat Flux (q") of 418 [kW|m^2] (≈ 42 [W|cm^2]) is obtained.
- This flux is not applied on the entire HR FW but only on the part covered by the solar image. Nevertheless, since a "partition device" which could limit the required relevant cooling effort only to the interested area is inconceivable, it has been conservatively assumed that the cooling system will act everywhere with the same principle and effectiveness.

Having just defined the Heat Flow (232 [W]), the increment of the coolant temperature (DT_water) through the HR can be readily calculated (Figure 7) because it is independent from the chosen heat exchange methodology.

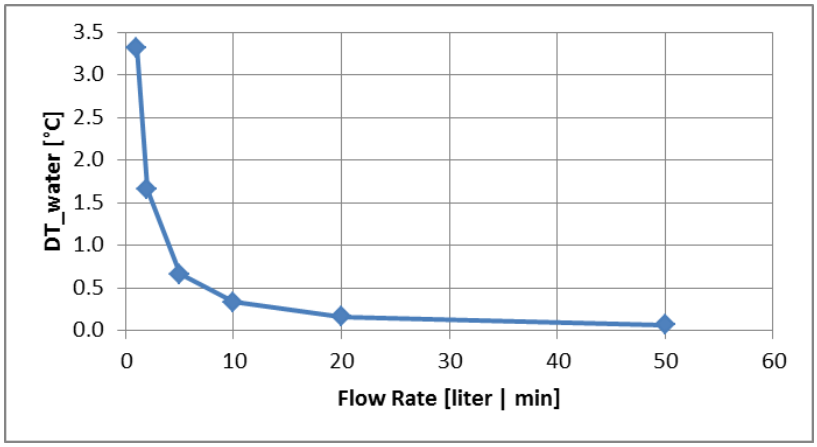

Figure 7 – Coolant Temperature Increment vs. Flow Rate

The opposite Delta-T must be provided by the chiller heat exchanger, and It must be noted that its required performance is absolutely not critical.

6.2 Design Constraints

The basics of the FW cooling process are shown Figure 8,

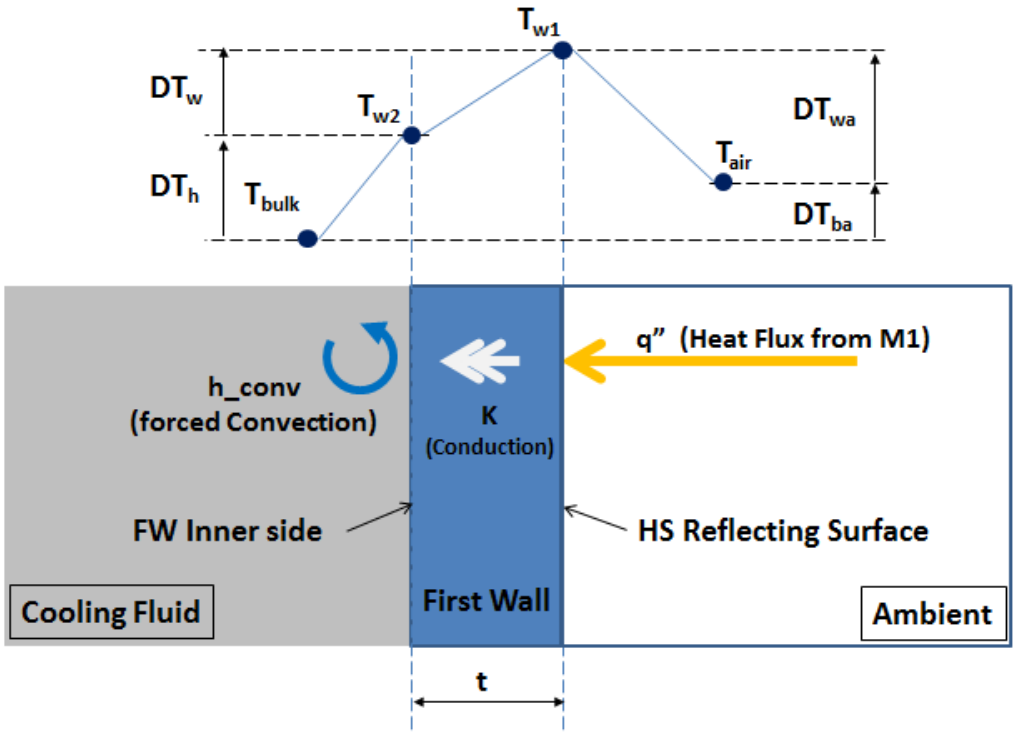

Figure 8 – HR FW cooling process

where:

T_{air}	Ambient temperature
T_{w1}	First Wall Outer Temperature (M1 side)
T_{w2}	First Wall backside Temperature
T_{bulk}	Coolant Temperature
DT_{Wa}	T_{W1}-T_{air}
DT_{ba}	T_{air}-T_{bulk}
DT_w	T_{W1}-T_{W2}
DT_h	T_{W2}-T_{bulk}
t	FW Thickness
K	FW Thermal Conduction
q"	Heat Flux
h_conv	Convective Heat Transfer Coefficient

Most of the Constraints are imposed on the Temperature Differences:

- **DT_{wa}** This is the most important parameter. The difference between the FW outer temperature and the Ambient air must be kept to a minimum in order to avoid the development of hot air plumes which degrade the Local Seeing (Optical Constraint)
- **DT_{ba}** The difference between Ambient and Bulk (coolant) temperatures must be enough small to avoid condensation of moisture over the feeders (coolant pipes)
- **DT_{w}** The difference between Outer and Inner FW temperatures must be enough small to avoid that the corresponding Thermal Gradient be harmful (Thermal Fatigue) for the FW structure.
- **DT_{h}** This is a derived parameter which, in turn, defines the HTC (Heat Transfer Coefficient) to be reached in order to satisfy the previous constraints.

The assumed values are reported in Table 4.

Design Variable	Value	Unit
DT_{w}	3.4	[°C]
DT_{ba}	8.0	[°C]
DT_{wa}	6.0	[°C]
DT_{h} (derived)	10.6	[°C]

Table 4 – Design Variable values

The material chosen for the FW is GLIDCOP™ Al-15, and the assumed FW thickness (**t**) is 3 [mm]. According to **Ref. 2**, GLIDCOP is widely used for high-heat-load components, such as photon absorbers, masks, and shutters of the third-generation light sources are subjected to intense thermal stress cycles from the high intensity x-ray beams. Basically, it is an *Al dispersion strengthened copper* primarily designed for applications requiring the highest elevated temperature strength, coupled with relatively high electrical and thermal conductivities. GLIDCOP™ Al-15 Thermo-Mechanical Properties (flat plate up to 10 [mm] thick) are reported in Table 5 (from **Ref. 2**)

ID	Property	Value	Units
K	Thermal conductivity	365	[W|m °C]
Cp	Specific Heat	390	[J|kg °C]
ρ	Density	8900	[kg|m^3]

Table 5 - GLIDCOP™ Al-15 Thermo-Mechanical Properties

Having already determined the reference q" Flux (418 [kW|m^2]), FW material and thickness, the Heat Transfer Coefficients can be readily determined (Table 6).

HTC	Value	Units	Note
h_conv	**39618**	[W|m^2 °C]	Coolant/FW backside convection
h_cond	121667	[W|m^2 °C]	Equivalent to FW conduction = k/t
H_tot	29886	[W|m^2 °C]	"Sum" (= 1/(1/h_conv+1/h_cond))

Table 6 – HTC

The key value (**h_conv ≈ 40,000 [W|m^2 °C]**) is an extremely high value and will require special techniques to be achieved (see next section).

6.3 Jet impingement

6.3.1 Single Jet Impingement

Reaching the required HTC by simply increasing the Reynolds number(i.e. high turbulence) in the current case (Figure 5) is not a practical solution since it implies reaching an extremely high coolant velocity. An alternative solution is to create very high turbulence (just were it is needed, that is on the backside of the FW) by sweeping away the laminar boundary layer. The concept is shown in Figure 9 (left). A single nozzle convoys the coolant against the backside of the heated plate. This technique is named "Jet Impingement" (JP). In the present case we speak of "Submerged Jet Impingement" since only the liquid phase is involved. High HTC is obtained, but it quickly decreases with the distance from the impinging jet axis (Figure 9 - right).

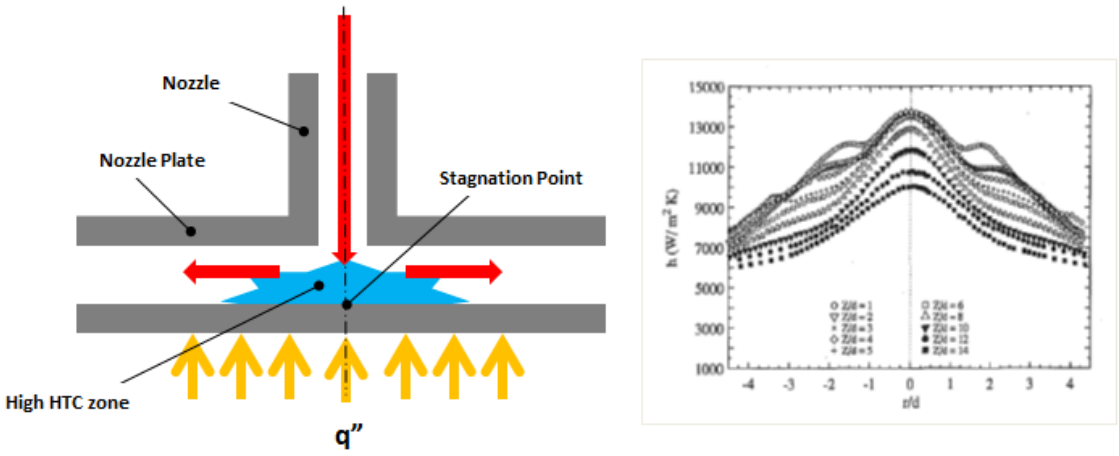

Figure 9 – Single Submerged Jet Impingement scheme

6.3.2 Multiple Jet Impingement

In order to cover wider areas (such as the FW backside plate) multiple nozzles are used (Figure 10).

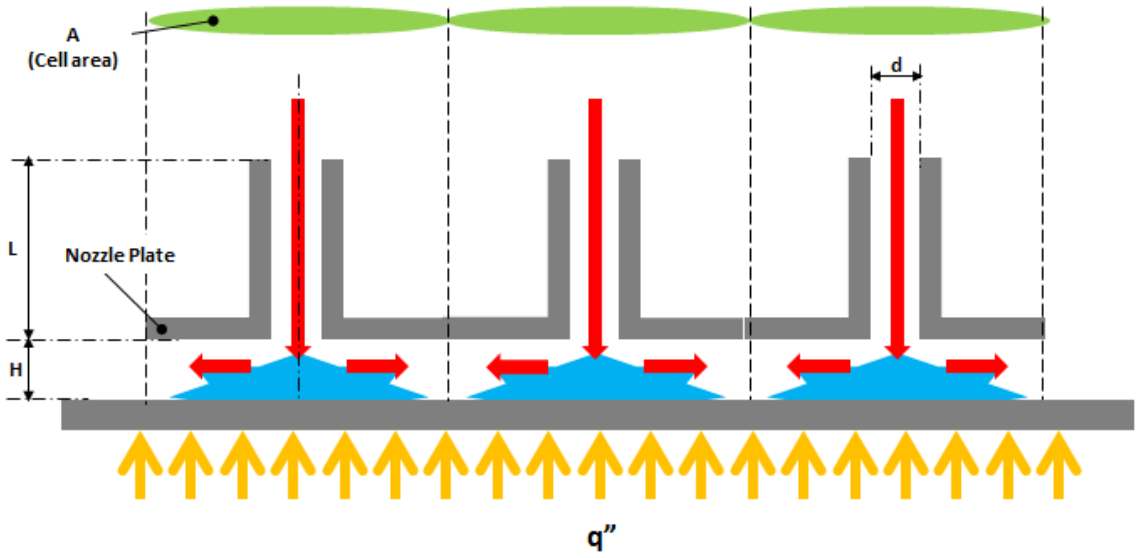

Figure 10 – Multiple Submerged Liquid Jet Impingement scheme

The Design Parameters of this arrangement are:

d	Nozzle diameter
L	Nozzle length
H	Height of the impingement chamber
A	Cell Area

The first three parameters drive the JP performance, that is the maximum valued of the HTC (at stagnation point) and the decreasing HTC profile as a function of the distance from the stagnation point itself. Since we are not interested in this profile, we will always think if terms of HTC average value over the "Cell area". The Cell area will determine the number of nozzle needed to meet the prescribed global performance (i.e. referred to the whole FW backside). It was demonstrated that very high HTC can be reached (200,000 [W|m^2°C], **Ref. 3**) at the price of extremely high coolant velocity in the nozzles (50 [m|s]) which results in impinged plate erosion and high coolant flow rates. The performance needed in the present case (40,000 [W|m^2°C]) will prevent such problems, because the expected velocity is lower by an order of magnitude.

6.3.3 Alternatives to Jet Impingement

At the beginning of the activity, another very efficient cooling technique was taken into account which is called "Hypervapotron". It basically consists in allowing a confined development of nucleate boiling inside slots, perpendicular to coolant flow. Examples of Hypervapotron channels are shown in Figure 11.

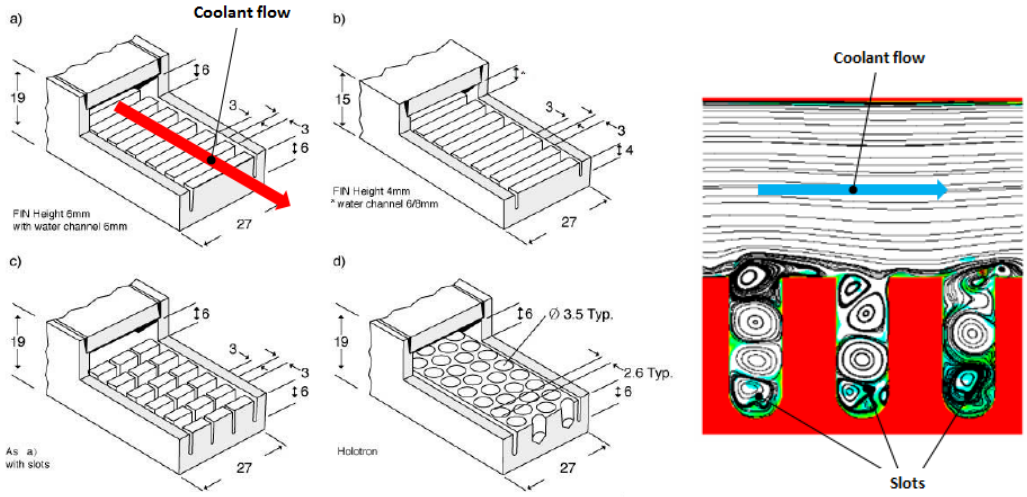

Figure 11 – Hypervapotron coolant channels

This technique is used where the absorption of huge heat fluxes (e.g. 20 [MW|m^2]) are involved, such as in the ITER divertor, and in the high-power Klystrons. In the present case a number of reasons discourage the use of Hypervapotron cooling system:

- Difficult to be analyzed/designed (extensive test required)
- The cooled wall must, in any case, reach the coolant saturation temperature (at least 100°C)
- Flow instabilities may occur
- Space (both in the wall thickness and along the coolant flow direction) is required which is not available in the HR.

In conclusion the Hypervapotron cooling mechanism has been discarded.

6.3.4 Jet Impingement Applicable Correlations

A number of correlations are available for the HTC evaluation in a single jet environment, while a few ones deals with multiple jets. All correlations provide averaged Nusselt number (Nu) as a function of Reynolds (Re) and Prandtl (Pr) number, and of the impingement zone geometry. The basic parameters involved are the following ones:

$$Nu = \frac{hd}{k} \qquad Re = \frac{\rho u d}{\mu} \qquad Pr = \frac{Cp\,\mu}{k}$$

Where:

h	Heat Transfer Coefficient (HTC)
d	Hydraulic Diameter (in this case: nozzle diameter)
u	coolant velocity (in this case: velocity in the nozzle)
k	coolant conductivity
Cp	coolant Specific Heat
μ	coolant Dynamic Viscosity

and:

A	Cell area
L	Nozzle length
H	Height of the impingement chamber

A tradeoff has been performed among some promising correlations (see next sections) aimed at determining the most conservative one (i.e. the one providing the lowest HTC) and the adopted solution is the one by Martin. The considered correlations provide an average value over the impinged area (the "Cell") which is, as previously mentioned, the information we need.

6.3.4.1 Chang correlation

Since the Multiple-Jet heat transfer correlations are admittedly affected by lack of experimental data, the single submerged flow correlations has been chosen (**Ref. 5**):

r/d ≤ 1.25 → $\overline{Nu} = 0.66 Re^{0.574} Pr^{0.4} \left(\frac{H}{d}\right)^{-0.106} \left[1 + \left(\frac{r}{d}\right)^{1.81}\right]^{-1}$

r/d ≤ 1.25 → $\overline{Nu} = 0.7017 Re^{0.574} Pr^{0.4} \left(\frac{H}{d}\right)^{-0.106} \left(\frac{r}{d}\right)^{-0.62}$

Where:

r	effective heat-source radius ($= \sqrt{A/\pi}$)
A	Cell area (Figure 10)

6.3.4.2 Garimella correlation

The "All fluids" correlation from **Ref. 6** is reported below:

$$\overline{Nu} = 1.179Re^{0.504}Pr^{0.441}\left(\frac{L}{d}\right)^{-0.071}\left(\frac{D_e}{d}\right)^{-0.283} + 1.211Re^{0.637}Pr^{0.441}\left(\frac{D_e}{d}\right)^{-1.062}(1-a_r)$$

Where:

D_e	Cell diameter ($= \sqrt{4A/\pi}$)
a_r	ratio of impingement area to heat-source area (= $(1.9d/D_e)^2$)
A	Cell area (Figure 10)

6.3.4.3 Rice correlation

The singular confined circular submerged jet correlation from **Ref. 7** is reported below:

$$\overline{Nu} = 0.160Re^{0.695}Pr^{0.4}\left(\frac{H}{d}\right)^{-0.52}\left(\frac{L}{d}\right)^{-0.11}$$

The provide value is averaged on a Cell area of 10x10 [mm^2] (the study was aimed at electronic chip cooling). When applied to smaller areas the expected value would be higher.

6.3.4.4 Martin correlation

The singular confined circular submerged jet correlation from **Ref. 7** is reported below:

$$\overline{Nu} = Pr^{0.42}\cdot G\cdot F$$

Where:

$$G = {}^{d}/_{R}\left\{\frac{1-1.1\,{}^{d}/_{r}}{1+0.1\left({}^{H}/_{d}-6\right){}^{d}/_{r}}\right\}$$

$$F = 2Re^{0.5}\left(1+\frac{Re^{0.55}}{200}\right)^{0.5}$$

r	effective heat-source radius ($= \sqrt{A/\pi}$)
A	Cell area (Figure 10)

6.3.5 Design Variables

The Design Variables, that is the parameters which can be changed to determine a possible solution of the Design problem, are listed below:

u water velocity inside the nozzle
d nozzle diameter
H distance between the nozzle plate and FW backside
r radius of the Cell

Additionally, the number of Feeders (the pipes running from the Supporting Ring to HR which feeds the HR itself) must be decided and must be considered a Design Variable too. The actual number is 2 (see 5.3), but that number will change (see below). Many tuples {U, d, H, r} can lead to a theoretically valid result, but only a few choices are valid under a technical point of view (feasibility). In order to refine the search for a valid technical solution, we assumed that such variables can assume only the prescribed values shown in Table 7:

Design Variable	Unit	Val 1	Val 2	Val 3	Val 4	Val 5
u	[m | s]	3	4	5	6	7
d	[mm]	1	1.5	2	2.5	3
H	[mm]	3	4			
r/d	[ ]	5	6	7	8	

Table 7 – Design Variable ranges

Having assumed the Design Constraint in Section 6.2, a "brute force" algorithm (nested loops) was used to calculate the corresponding HTC values. Solutions differing from the target value (40000 [W|m^2 °C]) for more than a given tolerance (-0.1%, +10%) have been discarded and a limited number of solutions was obtained. The resulting Coolant Flow Rate is in the range 9..15 [liter | min]. The flow rate determines the Coolant Velocity in the Feeders which have a fixed inner diameter of 3 [mm]. By assuming that the Coolant Velocity inside the Feeders must not exceed the value of 7 [m|s], the number of tubes, in parallel, which feed water to the HR must be 4 (see Table below).

Solution ID			id	8	6	5	2	1	9	7	4	3
			u	7	7	6	4	4	7	7	5	5
Design Variables			H	0.004	0.003	0.004	0.004	0.003	0.004	0.003	0.004	0.003
			d	0.001	0.001	0.001	0.001	0.001	0.0015	0.0015	0.0015	0.0015
HTC			R	0.006	0.006	0.005	0.004	0.004	0.0075	0.0075	0.006	0.006
			HTC	**41031**	**41751**	**43133**	**39773**	**40847**	**41681**	**42285**	**40063**	**40805**
Number of Nozzles			Nozzles	**27**	**27**	**40**	**62**	**62**	**17**	**17**	**27**	**27**
Mass Flow Rate			Gamma	0.15	0.15	0.19	0.19	0.19	0.21	0.21	0.24	0.24
# of tubes	Inner Diam.	Flow rate [kg | s]		**0.15**	**0.15**	**0.19**	**0.19**	**0.19**	**0.21**	**0.21**	**0.24**	**0.24**
[ ]	[mm]	[liter | min]		**8.89**	**8.89**	**11.29**	**11.67**	**11.67**	**12.59**	**12.59**	**14.29**	**14.29**
1	3	velocity [m | s]		21.0	21.0	26.7	27.6	27.6	29.8	29.8	33.8	33.8
2	3	velocity [m | s]		10.5	10.5	13.3	13.8	13.8	14.9	14.9	16.9	16.9
4	3	velocity [m | s]		**5.2**	**5.2**	**6.7**	**6.9**	**6.9**	**7.4**	**7.4**	**8.4**	**8.4**

Acceptable values for Coolant Velocity inside the Feeders

Table 8 – Selection of the Number of pipes feeding the HR

In conclusion, the Thermal-Hydraulic design has provided 5 possible solution, which are shown in the following Table.

		Sol	A	B	C	D	E
		id	8	6	5	2	1
		u	7	7	6	4	4
		H	0.004	0.003	0.004	0.004	0.003
		d	0.001	0.001	0.001	0.001	0.001
		R	0.006	0.006	0.005	0.004	0.004
		HTC	41031	41751	43133	39773	40847
		Nozzles	27	27	40	62	62
Feeders	Inner Diam.	Flow rate [kg | s]	0.15	0.15	0.19	0.19	0.19
[ ]	[mm]	[liter | min]	8.89	8.89	11.29	11.67	11.67
4	3	velocity [m | s]	5.2	5.2	6.7	6.9	6.9

Table 9 – Possible Thermal-Hydraulic Solution

The choice for the final solution will discussed in the Mechanical Design description.

6.3.6 HR Pressure Drop

The Pressure Drop across the HR for the various solution is reported in Table 10. Since distributed head loss along the nuzzle length can be neglected, only concentrated head loss have been evaluated by means of the following classical formula (**Ref. 8**):

$$\Delta P = \rho K \frac{u^2}{2}$$

Where:

ΔP	[Pa]	Pressure drop
R	[kg|m^3]	Coolant density
u	[m|s]	Coolant velocity in the nozzle
K	[ ]	K_{in} + K_{out}
$K_{in} = 0.5(1-\beta^2)$		sudden contractions coefficient (nozzle inlet)
$K_{out} = (1-\beta^2)^2$		sudden enlargement coefficient (nozzle outlet)
$\beta = \frac{d}{D}$		contraction or enlargement geometrical coefficient
d	[m]	Nozzle diameter
D	[m]	Cell diameter ($= \sqrt{4A/\pi}$)

Sol.	Flow Rate [liter|min]	u [m|s]	H [m]	d [m]	R [m]	ΔP [Pa]	ΔP [bar]
A	8.9	7	0.004	0.001	0.006	36260	**0.36**
B	8.9	7	0.003	0.001	0.006	36260	**0.36**
C	11.3	6	0.004	0.001	0.005	26504	**0.27**
D	11.7	4	0.004	0.001	0.004	11668	**0.12**
E	11.7	4	0.003	0.001	0.004	11668	**0.12**

Table 10 – HR Head Loss (pressure drop)

Even in the worst case (*B*, where ΔP = 0.36 [bar]) the Pressure Drop is not critical.

7 HR SYSTEM MECHANICAL DESIGN

7.1 Structural Assembly

Starting from the result of the Thermal-Hydraulic Design the a Mechanical Design which fulfills all the requirements has been developed (see Figure 12).

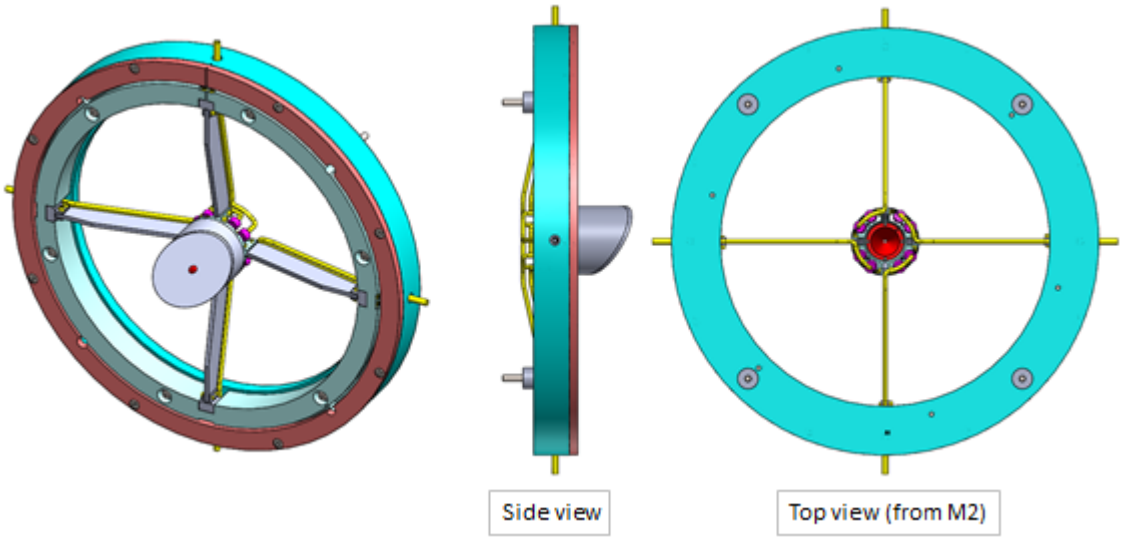

Figure 12 – HR structural assembly

Looking at Figure 13, it is apparent that the occlusion is slightly lower than the actual design and closer to the theoretical limit (the HR normal area, plus the four supporting beams).

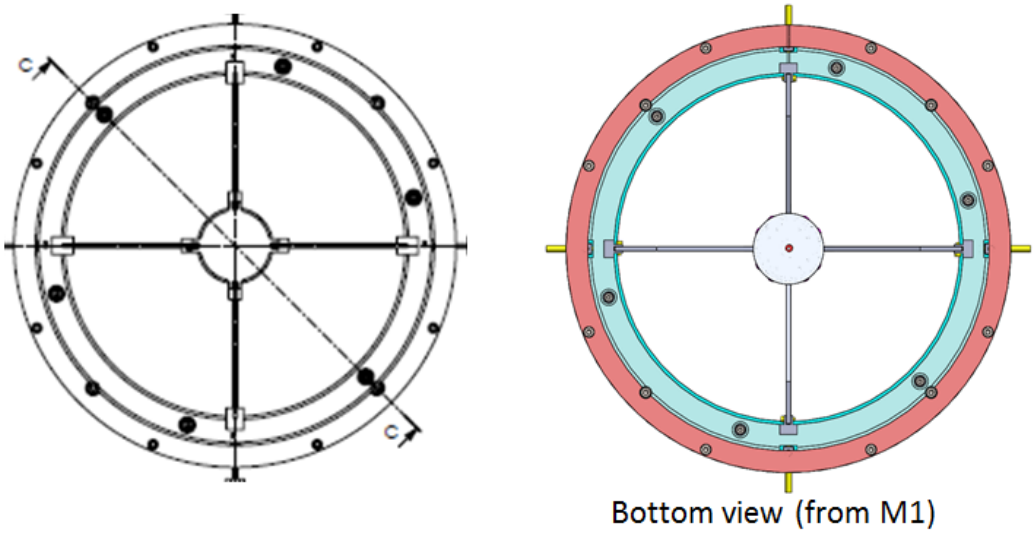

Figure 13 - HR System occlusion (left: actual design, right: new design)

The interface toward the telescope structure is not changed, and this guarantees the interchangeability of the new and old systems.

7.2 Hydraulic Assembly

A rough scheme of the new hydraulic circuit is reported in Figure 15. The major difference is encountered in the inner hydraulic circuit which features 8 feeders (i.e. 4 inlet and 4 outlet coolant pipes), arranged in a double cross scheme, entirely contained in the shadow of the 4 supporting beams (Figure 15). Special welded junctions are required to split the four outer feeders (interface to the existing coolant tubes) into eight smaller ones.

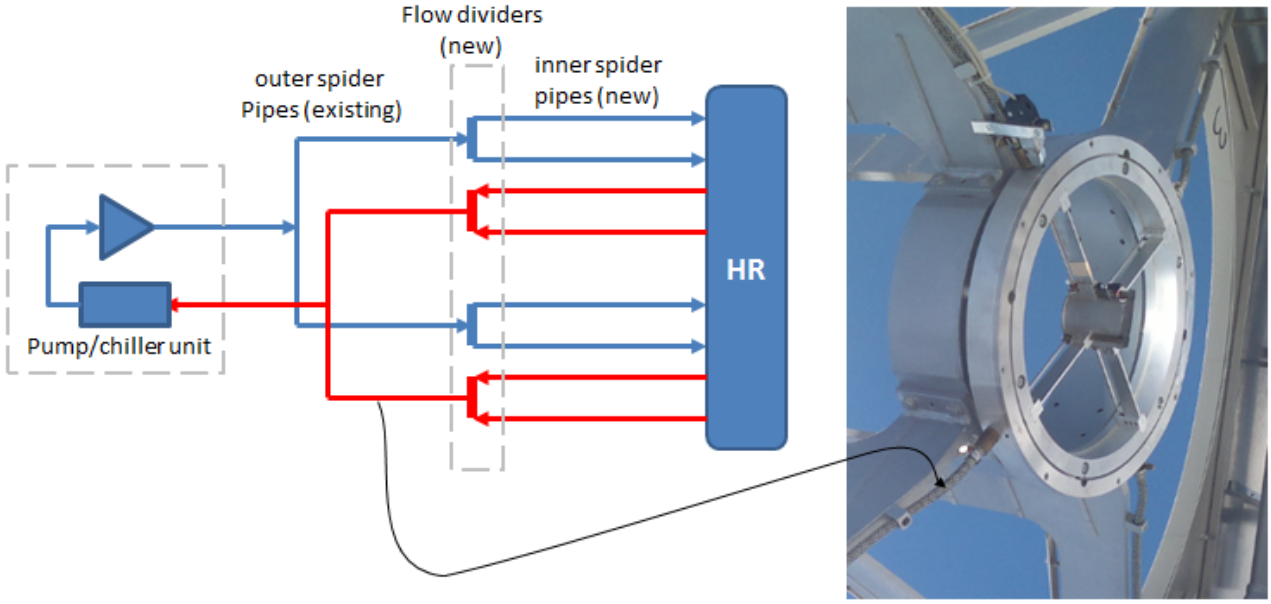

Figure 14 – HR Hydraulic Scheme

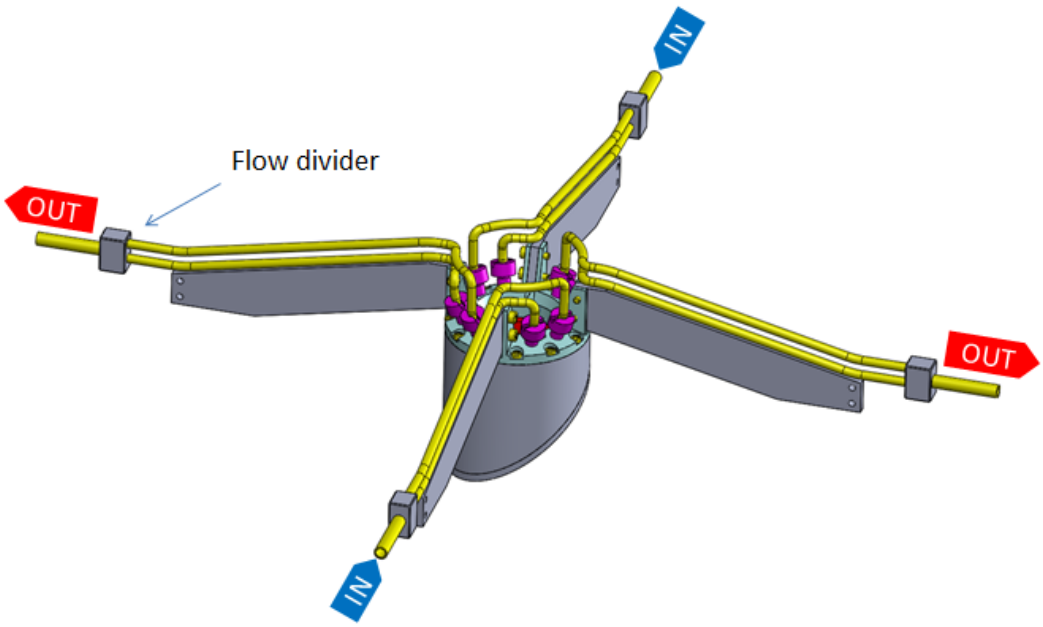

Figure 15 – HR Hydraulic assembly

The complexity of the feeder connections on the HR head (Figure 16) is apparent. Alternatives (such as brazed connections) are under technological evaluation.

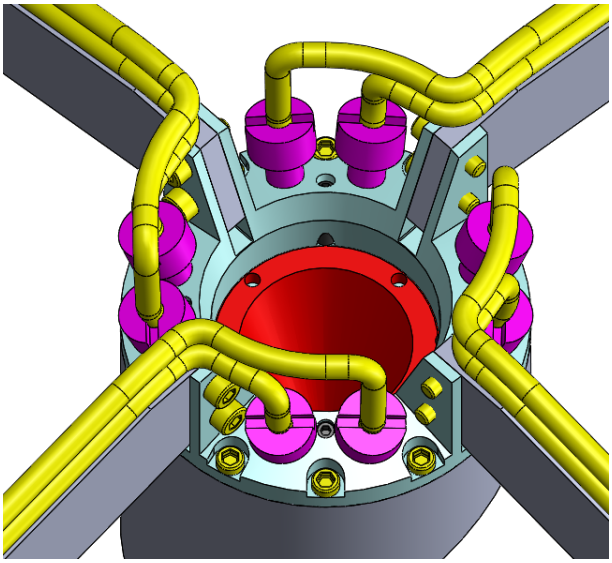

Figure 16 – Feeders Threaded connections on HR thread.

7.3 HR Mechanical design

The core of the whole system is the HR itself (Figure 18). It features a single cooling circuit which is made of a high pressure chamber, the JP plate, and the low pressure chamber. Nozzles across the boundary between high and low pressure chambers are apparent.

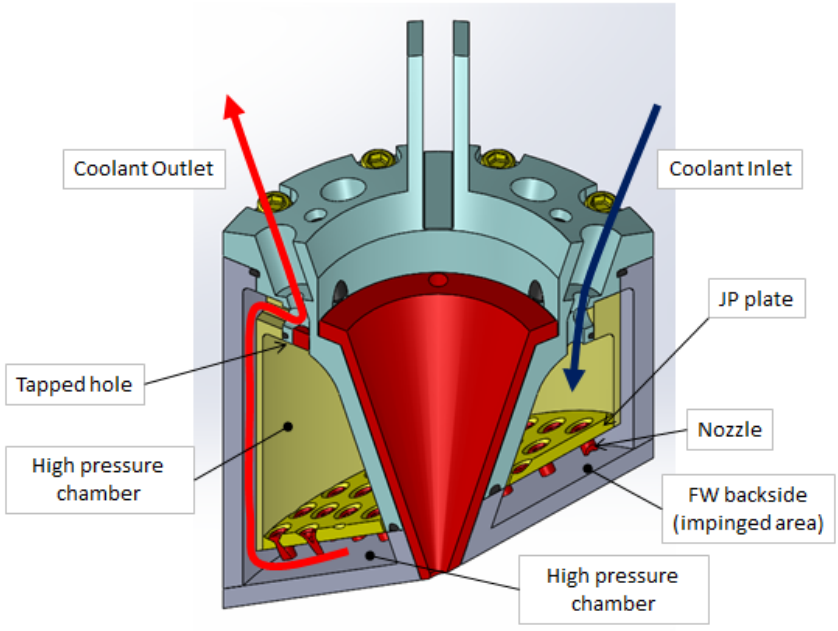

Figure 17 – HR Hydraulic Scheme

The red inner cone is interchangeable with other ones with different diaphragm hole diameters. It has been demonstrated (see Section 8) that this solution allows a sustainable edge temperature.

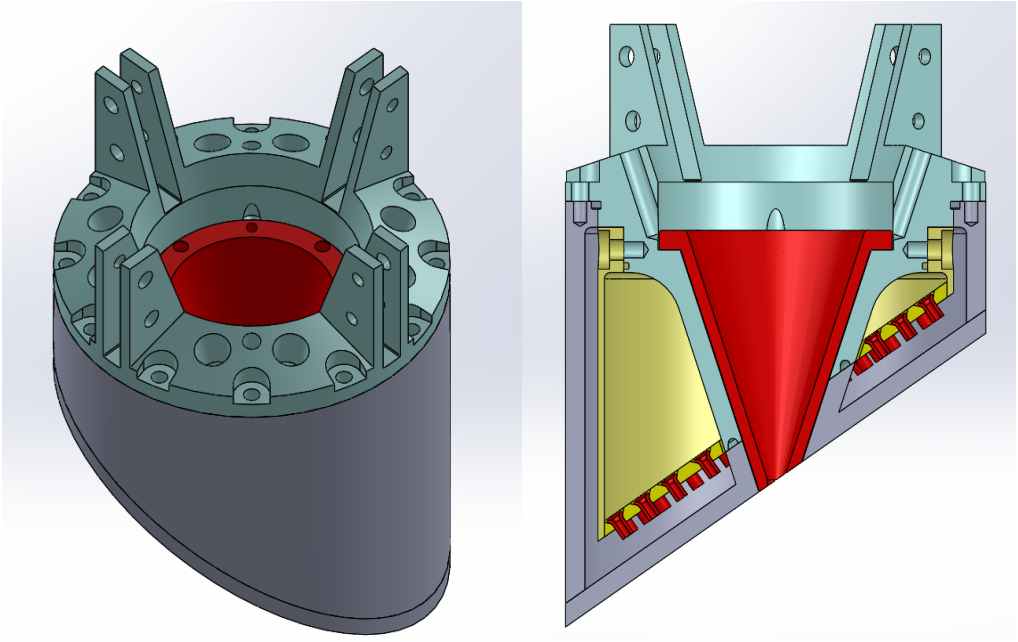

Figure 18 – HR Structure

An exploded view of the HR is reported in Figure 19, which summarize the mount/dismount procedure.

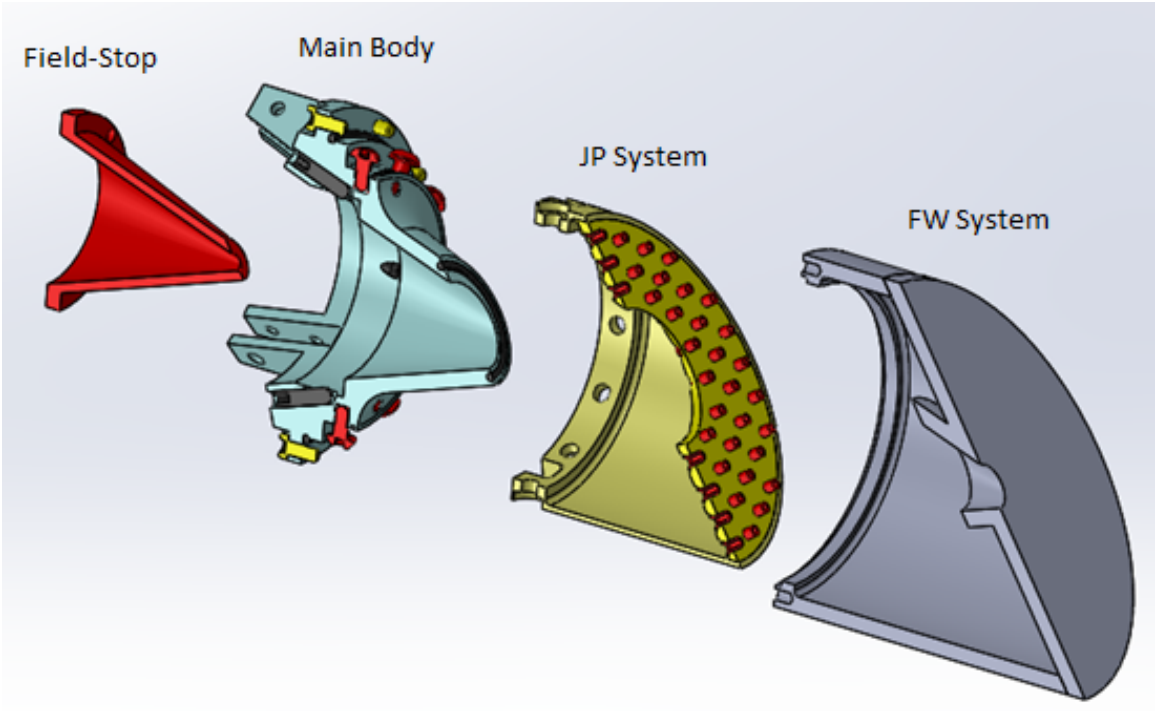

Figure 19 – HR Exploded View

The more complex part of the HR is the whole system is the HR Body (see section and view in the figures below), which is made of AISI316 stainless steel.

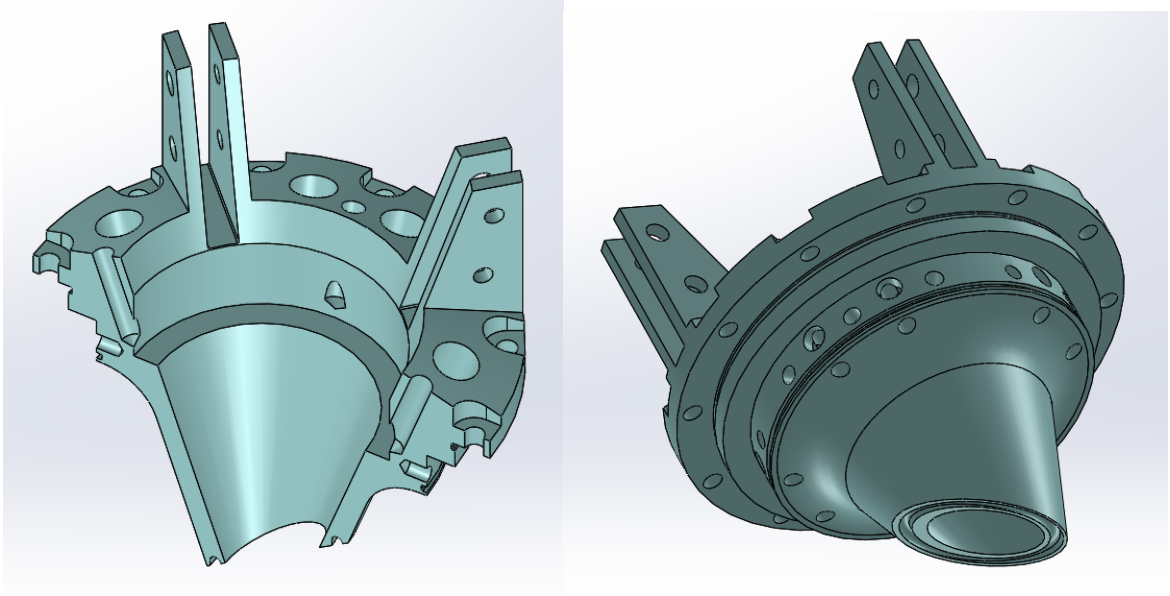

The JP body and the reported nozzles(on the left figure below) are made of AISI316 too. The HR Lower body (on the right figure below) includes the FW (the inclined surface) and is made of GLIDCOP.

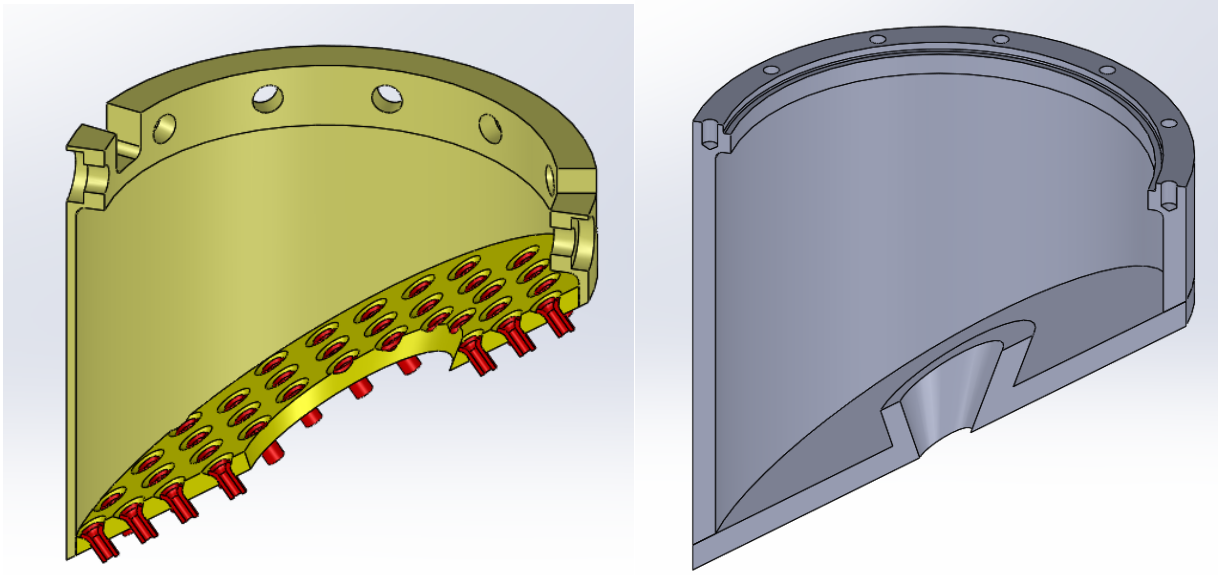

The actual design (“detailed design”) is now under technological revision and will be soon finalized into the final “constructive design”.

8 FIELD-STOP THERMAL AND MECHANICAL DESIGN

The Field-Stop (FS) is a HR subsystem which features a hollow cone which can be easily replaced by one with a different hole diameter (Figure 20).

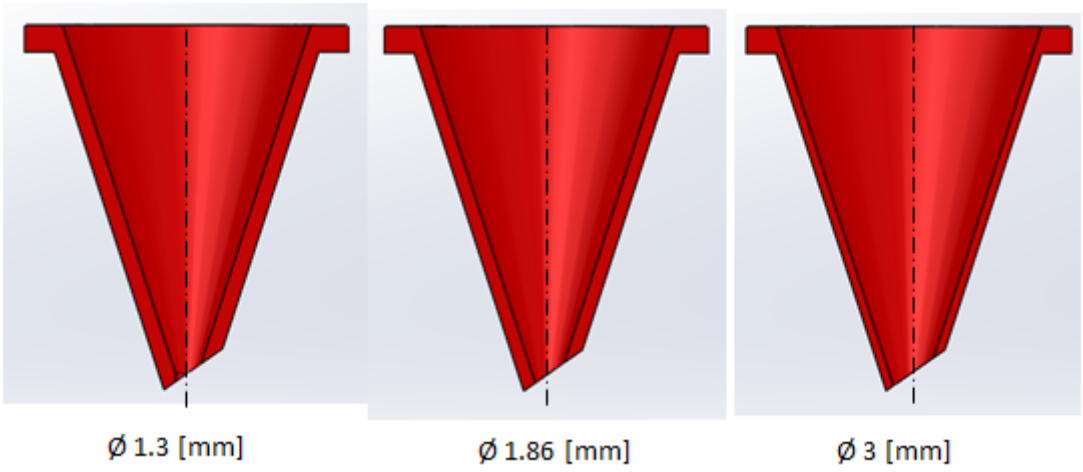

Figure 20 – HR interchangeable Field-Stops

Four Socket Set Screws are used to lock the FS inside the HR body (Figure 21). Centering pins, and additional threaded holes for disengaging and lifting are provided as well. Some Thermally Conductive Grease must be put in the small gap (1/10 [mm]) between the FS and the HR body.

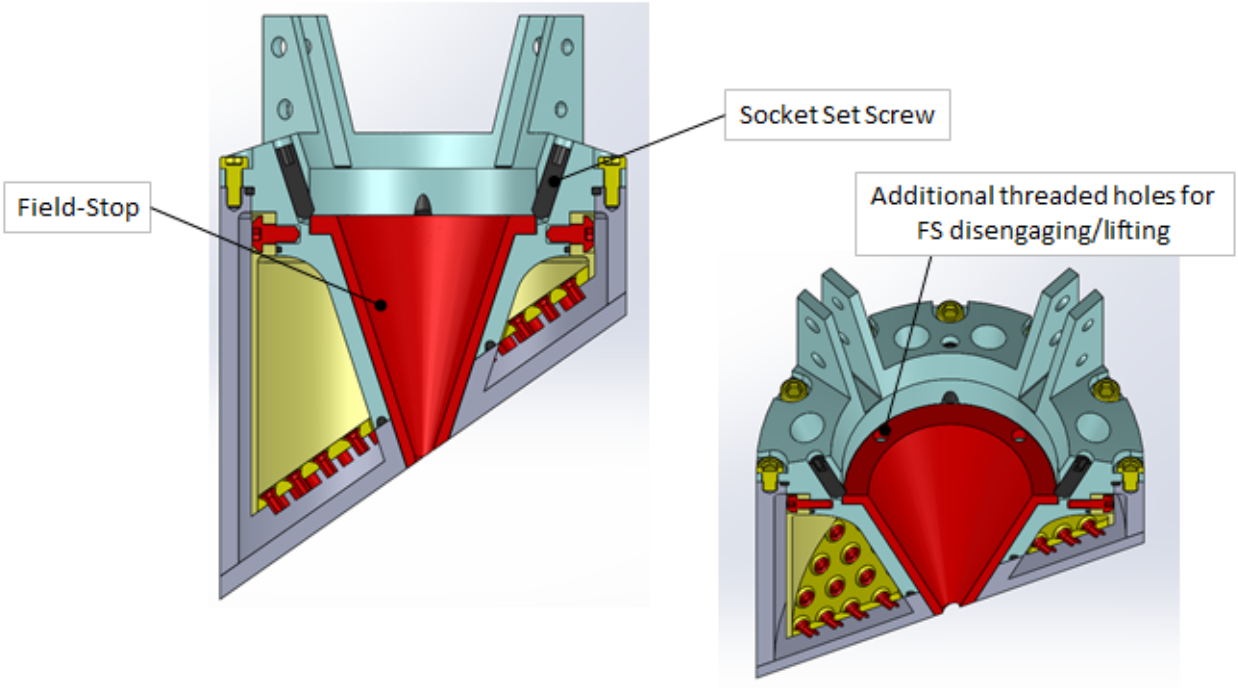

Figure 21 – FS Locking System

This arrangement withstands the high thermal loads which characterize the FW because the Sun-exposed area is limited to the annulus cut by the FW plane. In short, the heat power impinges the very small annulus area and will by dissipated by the entire cone external surface (that's the purpose of the conductive grease). In order to assess the subsystem performance a very conservative thermal analysis has been done by assuming that the thermal contact is limited to the upper ring (Figure 22).

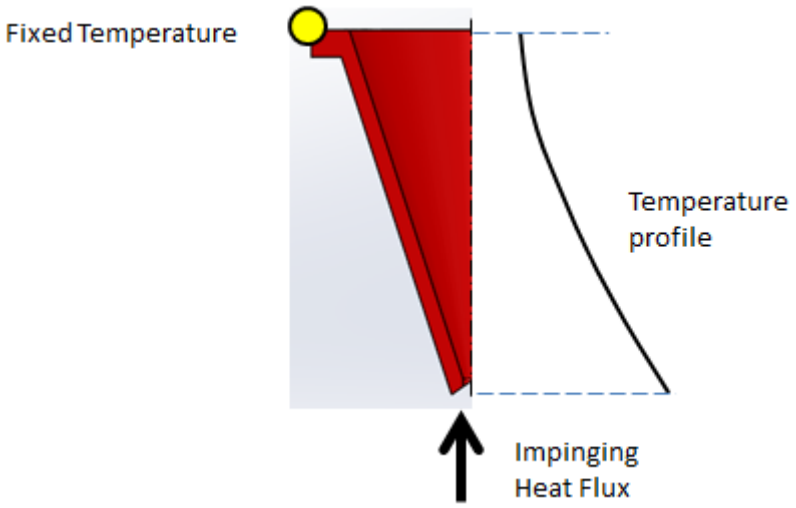

Figure 22 - FS Thermal Analysis Scheme

By assuming a Heat Flux[1] of 650 [kW|m^2], and a Fixed Temperature of 25 [°C], the evolution of the Temperature profile shown in Figure 23 has been determined.

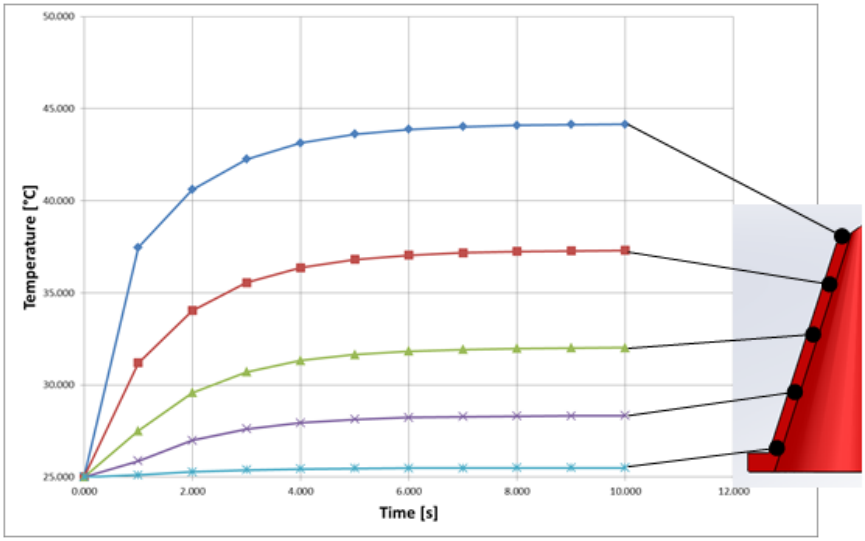

Figure 23 – FS Temperature Profile Evolution

The annulus temperature is just 20 [°C] higher than the Fixed Temperature values, which implies that, even under very conservative boundary conditions, no thermal problem will affect the FS structure.

[1] In the axisymmetric thermal analysis a not reduced valued was assumed